Article

Acylphloroglucinol Derivatives from *Garcinia multiflora* with Anti-Inflammatory Effect in LPS-Induced RAW264.7 Macrophages

Lin-Yang Cheng [1], **Yun-Chen Tsai [2]**, **Shu-Ling Fu [2,†]**, **Ming-Jen Cheng [3]**, **Ping-Jyun Sung [4]**, **Mei-Ing Chung [1,*,†]** and **Jih-Jung Chen [5,6,*]**

[1] School of Pharmacy, College of Pharmacy, Kaohsiung Medical University, Kaohsiung 807, Taiwan; u100830009@kmu.edu.tw

[2] Institute of Traditional Medicine, National Yang-Ming University, Taipei 112, Taiwan; tyc202006@gmail.com (Y.-C.T.); slfu@ym.edu.tw (S.-L.F.)

[3] Bioresource Collection and Research Center (BCRC), Food Industry Research and Development Institute (FIRDI), Hsinchu 300, Taiwan; cmj@firdi.org.tw

[4] National Museum of Marine Biology and Aquarium, Pingtung 944, Taiwan; pjsung@nmmba.gov.tw

[5] Faculty of Pharmacy, School of Pharmaceutical Sciences, National Yang-Ming University, Taipei 112, Taiwan

[6] Department of Medical Research, China Medical University Hospital, China Medical University, Taichung 404, Taiwan

[*] Correspondence: meinch@kmu.edu.tw (M.-I.C.); chenjj@ym.edu.tw (J.-J.C.); Tel.: +886-7-312-1101 (ext. 2672) (M.-I.C.); +886-2-2826-7195 (J.-J.C.)

[†] These authors contributed equally to this work.

check for updates

Abstract: Two new acylphloroglucinol derivatives, 13,14-didehydroxygarcicowin C (**1**) and 13,14-didehydroxyisoxanthochymol (**2**), have been isolated from the stems of *Garcinia multiflora*, together with seven known compounds (**3–9**). The structures of new compounds **1** and **2** were elucidated by MS and extensive 1D/2D NMR spectroscopic analyses. Among the isolates, 13,14-didehydroxy-isoxanthochymol (**2**) and sampsonione B (**3**) exhibited inhibition against lipopolysaccharide (LPS)-induced NF-κB activation in macrophages at 30 μM with relative luciferase activity values (inhibitory %) of 0.75 ± 0.03 (24 ± 4%) and 0.12 ± 0.03 (88 ± 4%), respectively. Additionally, sampsonione B (**3**) reduced LPS-induced nitric oxide (NO) production in murine RAW264.7 macrophages and did not induce cytotoxicity against RAW 264.7 cells after 24 h treatment. Compound **3** is worth further investigation and may be expectantly developed as an anti-inflammatory *drug candidate*.

Keywords: *Garcinia multiflora*; Guttiferae; structure elucidation; nuclear factor κB; nitric oxide; anti-inflammatory activity

1. Introduction

Garcinia multiflora Champ. (Guttiferae) is a small evergreen tree [1], usually growing 5–15 m tall, distributed in South China, Taiwan, and Hong Kong. Fruit from this plant is edible. In Taiwan, the genus *Garcinia* is represented by three species, *Garcinia multiflora*, *Garcinia linii*, and *Garcinia subelliptica*. Xanthones [2–5], acylphloroglucinols [6–9], flavanones [10], and their derivatives are distributed in plants of the genus *Garcinia*. Multiple activities have been reported for these derivatives such as cytotoxic [3–5], anti-microbial [2], anti-inflammatory [6–8], anti-oxidant [2], and AChE enzymes inhibitory activities [10]. Aberrant inflammation is associated with many diseases such as arthritis, asthma, and cancer [11]. Among immune cells, macrophages are highly

responsive to lipopolysaccharide (LPS) and activated macrophages produce multiple pro-inflammatory molecules (such as nitric oxide (NO)). Nuclear factor κB (NF-κB) [12,13] is a transcription factor mediating inflammatory responses and known as a drug target for anti-inflammatory strategy. In our research on the anti-inflammatory constituents of Formosan plants, numerous species had been screened for inhibitory activity on LPS-induced NF-κB activation, and *G. multiflora* was found to be an active species. Phytochemical investigations on the stems of *G. multiflora* has resulted in the isolation of two new acylphloroglucinol derivatives, 13,14-didehydroxygarcicowin C (**1**) and 13,14-didehydroxy-isoxanthochymol (**2**), along with seven known compounds. We evaluated the anti-inflammatory effect of the isolated compounds in LPS-stimulated RAW264.7 macrophages and found that 13,14-didehydroxyisoxanthochymol (**2**) and sampsonione B (**3**) decreased NF-κB activity. Moreover, sampsonione B (**3**) inhibited the production of nitric oxide (NO) in LPS-activated macrophages. In this article, the structural elucidation of **1** and **2** and the inhibitory activity of the isolates on LPS-induced NF-κB activation are described.

2. Results and Discussion

2.1. Isolation and Structural Elucidation

Chromatographic isolation and purification of the EtOAc-soluble fraction of a MeOH extract of stems of *G. multiflora* on a silica gel column and preparative thin-layer chromatography (TLC) obtained two new (**1** and **2**) and seven known compounds (**3**–**9**) (Figure 1).

13,14-Didehydroxygarcicowin C (**1**) was obtained as colorless, amorphous powder. The ESI-MS (Figure S1) displayed the quasi-molecular ion $[M + H]^+$ at m/z 569, implying a molecular formula of $C_{38}H_{49}O_4$, which was confirmed by the HR-ESI-MS (m/z 569.36284 $[M + H]^+$, calcd 569.36254) (Figure S2) and by the ^1H, ^{13}C, and DEPT NMR data. The presence of carbonyl groups was revealed by the bands at 1729, 1682, and 1645 cm^{-1} in the IR spectrum and was confirmed by signals at δ_C 209.0, 193.8, and 193.1 in the ^{13}C NMR spectrum. The ^1H and ^{13}C NMR spectrum (Table 1) (Figures S3 and S4) of **1** showed signals for an acylphloroglucinol derivative based on the presence of a 2,2-dimethylbicyclo[3.3.1]nonane ring system, a benzoyl group, two isoprenyl groups, and another C_{10} unit (C-29 through C-38). The ^1H NMR data of **1** were similar to those of garcicowin C (Figure 2) [14], except that the benzoyl group [δ_H 7.38 (2H, t, J = 7.5 Hz, H-13, and H-15), 7.50 (1H, t, J = 7.5 Hz, H-14), and 7.77 (2H, d, J = 7.5 Hz, H-12, and H-16)] of **1** replaced the 3,4-dihydroxybenzoyl group of garcicowin C. This was supported by the HMBC correlations observed between H-12 (δ_H 7.77) and C-10 (δ_C 193.1), C-14 (δ_C 133.0), and C-16 (δ_C 128.7). The relative configuration of **1** was deduced from the NOESY cross-peaks (Figure 3) of H-17/H-22, H-22/H-6, H$_\alpha$-7/H-22, H$_\alpha$-7/H-29, H$_\alpha$-29/H-35, and H-34/H-32. Consequently, H-6, the isoprenyl group at C-4, and the bond between C-8 and C-29 are on the α-side, and H-34 and the prop-1-en-2-yl group at C-30 are on the β-side of **1**. According to the data of the ^1H–^1H COSY (Figure S5) and NOESY (Figure S6) spectra, a computer-created 3D structure was established by applying the above-mentioned molecular modeling program with MM2 force-field calculations for energy minimization. The NOESY experiment of **1** showed selected cross-peaks as shown in the 3D drawing (Figure 4). The calculated distances between H-17/H-22 (2.248 Å), H-22/H-6 (2.304 Å), H$_\alpha$-7/H-29 (2.281 Å), H$_\alpha$-29/H-35 (2.552 Å), and H-34/H-32 (2.364 Å) are all less than 4.00 Å; this corresponds with the well-defined NOESY examined for each of the proton pairs. The absolute configuration of **1** was indicated by CD Cotton effects at 311 ($\Delta\varepsilon$ + 2.1), 267 ($\Delta\varepsilon$ − 8.5), 223 ($\Delta\varepsilon$ + 5.2) nm in analogy with garcicowin C [15]. The full assignment of ^{13}C and ^1H NMR resonances was substantiated by DEPT, ^1H–^1H COSY, NOESY (Figure 3), HMBC (Figure 3) (Figure S7), and HSQC (Figure S8) experiments. On the basis of the above evidence, the structure of **1** was established as 13,14-didehydroxygarcicowin C.
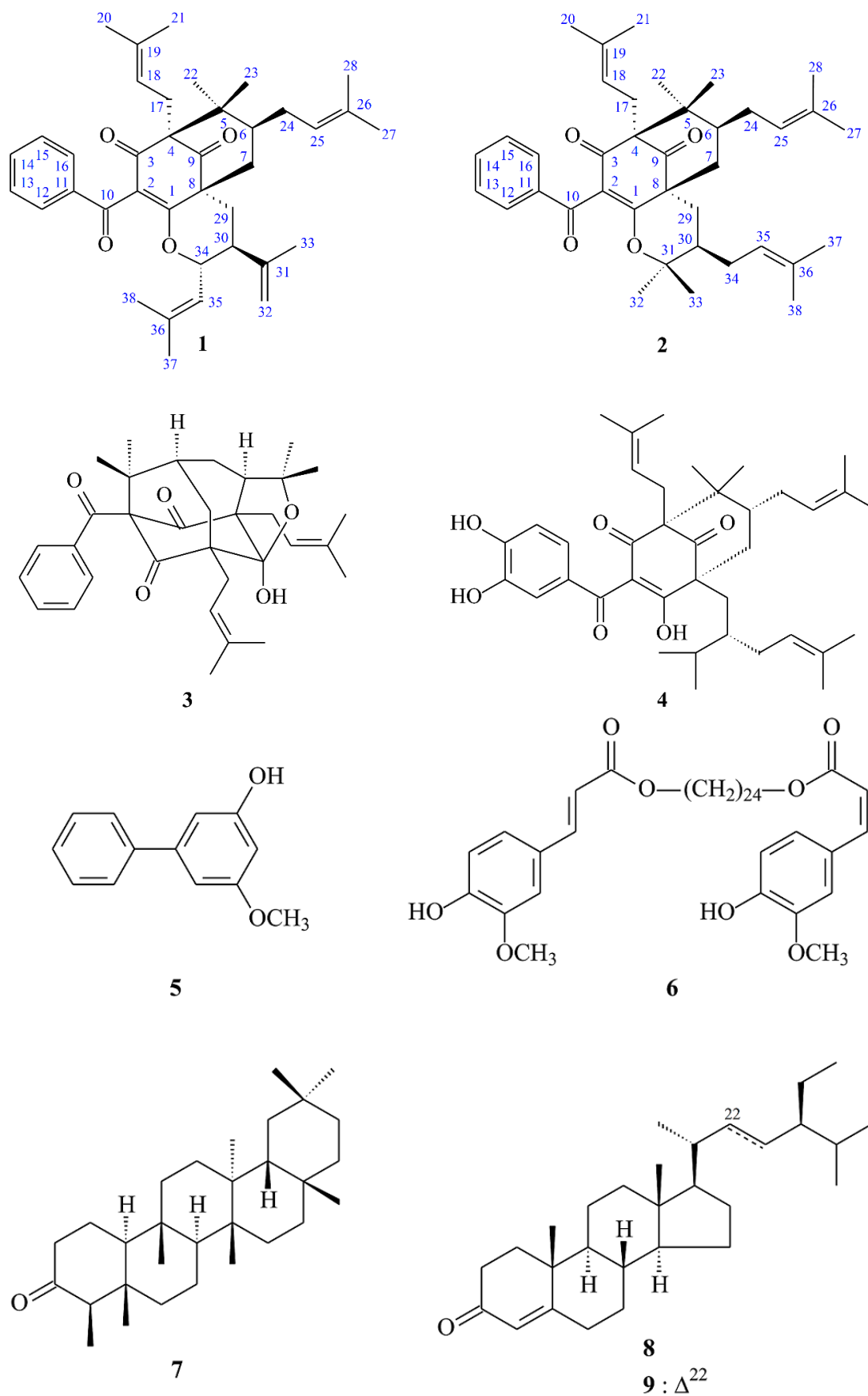
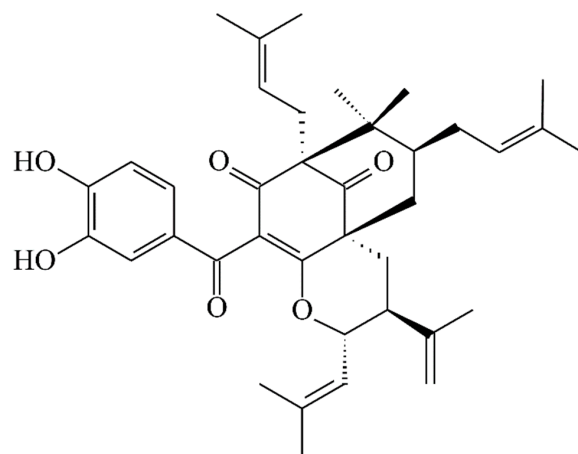**Figure 1.** The chemical structures of compounds **1**–**9** isolated from *Garcinia multiflora*.

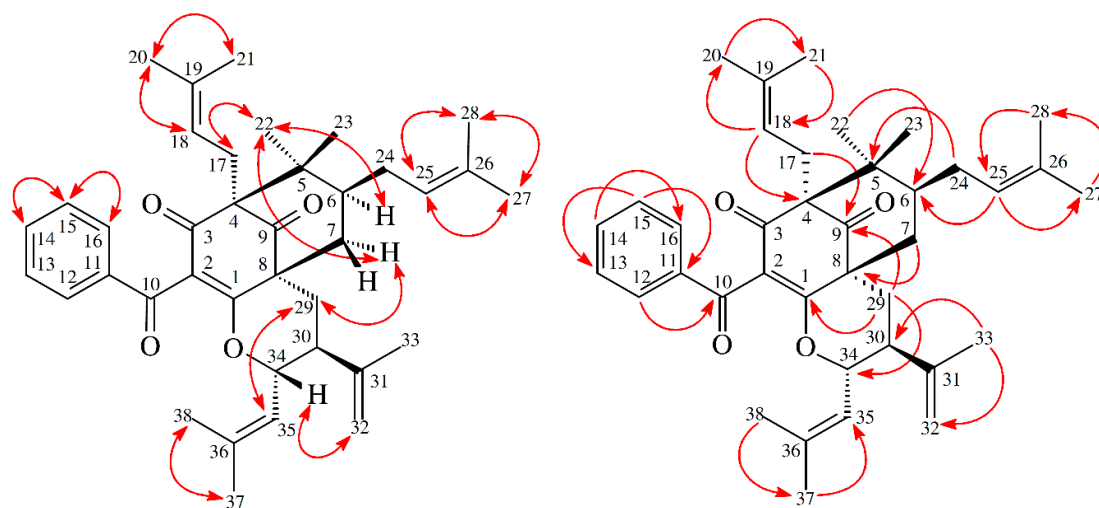**Figure 2.** The chemical structure of garcicowin C.

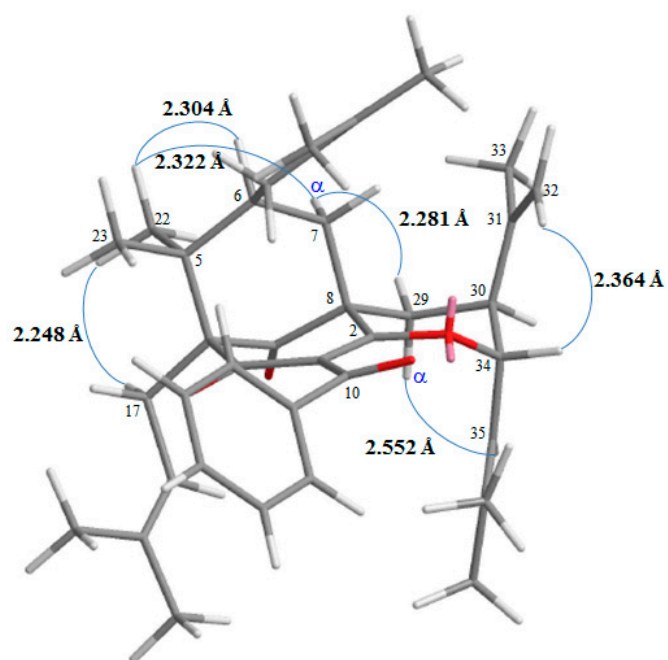**Figure 3.** Key NOESY (⟵⟶) and HMBC (⟶) correlations of **1**.

Figure 4. Selected NOESY correlations and relative configuration of **1**.

Table 1. ^{1}H NMR (500 MHz) and ^{13}C NMR (125 MHz) data for compounds **1** and **2** in CDCl$_3$.

Position	1		2	
	δ_C, type	δ_H (*J* in Hz)	δ_C, type	δ_H (*J* in Hz)
1	170.8, C		171.5, C	
2	129.1, C		125.3, C	
3	193.8, C		193.7, C	
4	69.2, C		68.3, C	
5	46.7, C		46.3, C	
6	46.4, CH	1.51, m	46.2, CH	1.45, m
7	38.1, CH$_2$	2.60, d (14.5)	39.5, CH$_2$	2.28, d (14.5)
		1.89, dd (14.5, 7.5)		1.98, dd (14.5, 7.0)
8	48.1, C		51.2, C	
9	209.0, C		207.1, C	
10	193.1, C		193.8, C	
11	137.5, C		137.5, C	
12	128.7, CH	7.77, d (7.5)	128.8, CH	7.72, d (7.5)
13	128.3, CH	7.38, t (7.5)	128.3, CH	7.36, t (7.5)
14	133.0, CH	7.50, t (7.5)	132.9, CH	7.49, t (7.5)
15	128.3, CH	7.38, t (7.5)	128.3, CH	7.36, t (7.5)
16	128.7, CH	7.77, d (7.5)	128.8, CH	7.72, d (7.5)
17	25.3, CH$_2$	2.66, dd (13.5, 8.0)	25.5, CH$_2$	2.68, dd (14.0, 8.5)
		2.47, m		2.43, dd (14.0, 5.0)
18	119.8, CH	4.91, br t (8.0)	119.8, CH	4.95, dd (8.5, 5.0)
19	134.6, C		134.7, C	
20	26.1, CH$_3$	1.62, s	26.2, CH$_3$	1.62, s
21	18.1, CH$_3$	1.56, s	18.0, CH$_3$	1.58, s
22	26.8, CH$_3$	1.00, s	26.8, CH$_3$	0.98, s
23	22.3, CH$_3$	1.18, s	22.5, CH$_3$	1.17, s
24	29.3, CH$_2$	2.53, m	29.3, CH$_2$	2.65, m
		2.23, m		2.19, m
25	124.9, CH	4.94, br t (7.5)	124.9, CH	4.90, br t (7.0)
26	133.1, C		133.1, C	
27	26.0, CH$_3$	1.71, s	26.0, CH$_3$	1.70, s
28	18.2, CH$_3$	1.67, s	18.1, CH$_3$	1.69, s
29	33.2, CH$_2$	2.32, t (14.0)	28.4, CH$_2$	3.05, dd (14.0, 3.5)
		1.75, dd (14.0, 2.5)		0.92, m
30	42.8, CH	2.46, m	42.8, CH	1.39, m
31	143.5, C		86.4, C	
32	113.9, CH$_2$	4.80, s	28.5, CH$_3$	0.83, s
		4.84, s		
33	20.3, CH$_3$	1.66, s	21.3, CH$_3$	1.23, s
34	79.7, CH	4.20, t (9.0)	29.6, CH$_2$	2.03, m
				1.78, m
35	121.4, CH	5.01, br d (9.0)	121.4, CH	5.19, br t (6.5)
36	141.7, C		133.7, C	
37	25.7, CH$_3$	1.61 s	25.8, CH$_3$	1.77 s
38	17.8, CH$_3$	1.10 s	18.1, CH$_3$	1.60 s

13,14-Didehydroxyisoxanthochymol (**2**) was isolated as a colorless amorphous powder with molecular formula C$_{38}$H$_{50}$O$_4$ as established by ESI-MS (Figure S9) and HR-ESI-MS (Figure S10), revealing an [M + H]$^+$ ion at *m/z* 571.37822 (calcd for C$_{38}$H$_{51}$O$_4$, 571.37819). The presence of carbonyl groups was revealed by the bands at 1724, 1675, and 1637 cm^{-1} in the IR spectrum and was confirmed by signals at δ_C 207.1, 193.8, and 193.7 in the ^{13}C NMR spectrum. The ^{1}H- and ^{13}C NMR spectrum (Table 1) (Figures S11 and S12) of **2** showed signals for an acylphloroglucinol derivative based on the presence of a 2,2-dimethylbicyclo[3.3.1]nonane ring system, a benzoyl group, three isoprenyl groups, and another C$_5$ unit (C-29 through C-33). The NMR data of **2** was similar to those of isoxanthochymol (Figure 5) [16], except that the benzoyl group [δ_H 7.36 (2H, t, *J* = 7.5 Hz, H-13 and H-15), 7.49 (1H, t,

J = 7.5 Hz, H-14), and 7.72 (2H, d, *J* = 7.5 Hz, H-12 and H-16)] of **2** replaced the 3,4-dihydroxybenzoyl group of isoxanthochymol [16]. This was supported by the HMBC correlations observed between H-12 (δ_H 7.72) and C-10 (δ_C 193.8), C-14 (δ_C 132.9), and C-16 (δ_C 128.8). The relative configuration of **2** was determined by NOESY cross-peaks (Figure 6) of H-17/H-22, H-22/H-6, H_α-7/H-22, H_α-7/H-29, H_α-29/H-30, and H_β-7/H-34. Consequently, H-6, the isoprenyl group at C-4, and the bond between C-8 and C-29 are on the α-side, and the isoprenyl group at C-6 and the isoprenyl group at C-30 are on the β-side of **2**. A computer-created 3D structure (Figure 7) was established by applying the above-mentioned molecular modeling program with MM2 force-field calculations for energy minimization. The calculated distances between H-17/H-22 (2.301 Å), H-22/H-6 (2.274 Å), H-22/H_α-7 (3.109 Å), H_α-29/H-30 (2.546 Å), H_β-7/H-34 (2.128 Å), and H_β-7/H-24 (3.246 Å) are all less than 4.00 Å; this corresponds with the well-defined NOESY observed for each of the proton pairs. The absolute configuration of **2** was confirmed by the similar CD Cotton effects [270 (Δε + 13.6), 224 (Δε − 8.4) nm] compared with analogous benzoylphloroglucinol derivative, isoxanthochymol [16]. The structure elucidation of **2** was confirmed by ^{1}H–^{1}H COSY (Figure S13) and NOESY (Figure 6) (Figure S14) techniques and ^{13}C NMR assignments were supported by DEPT, HMBC (Figure 6) (Figure S15), and HSQC (Figure S16) experiments. According to the above evidence, the structure of **2** was established as 13,14-didehydroxyisoxanthochymol.
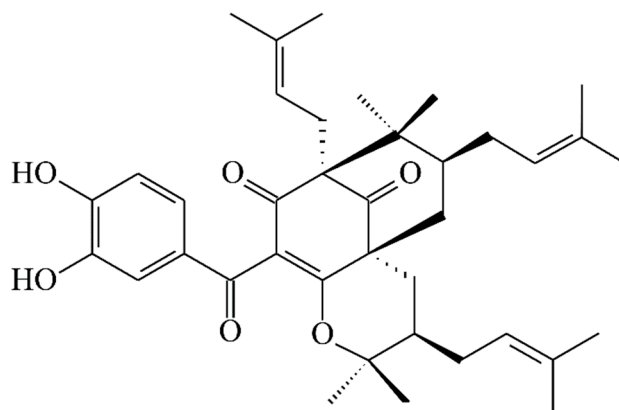

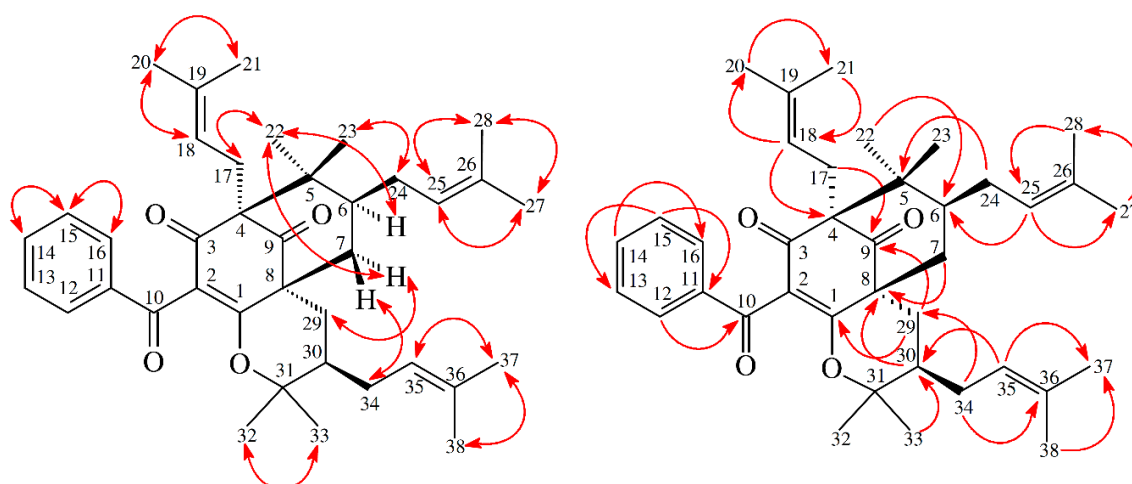**Figure 5.** The chemical structure of isoxanthochymol.

Figure 6. Key NOESY (⟵⟶) and HMBC (⌒⟶) correlations of **2**.
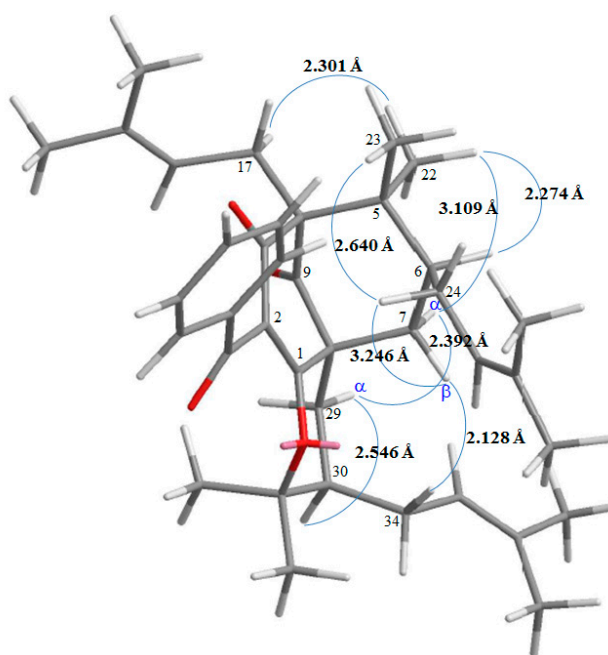
Figure 7. Selected NOESY correlations and relative configuration of **2**.

2.2. Structure Identification of the Known Isolates

The known isolated compounds were easily identified by a comparison of spectroscopic and physical data (^{1}H NMR, UV, MS, [α]$_D$, and IR) with corresponding authentic samples or literature values, and this included two acylphloroglucinol derivatives, sampsonione B (**3**) [17] and garcinol (**4**) [16], a biphenyl derivative, 3-hydroxy-5-methoxybiphenyl (**5**) [18], a ferulic acid ester derivative, 1,24-tetracosanediol diferulate (**6**) [19], a triterpene, friedelan-3-one (**7**) [20], and a mixture of steroids, β-sitostenone (**8**) [21] and stigmasta-4,22-dien-3-one (**9**) [22].

2.3. Biological Studies

NF-κB [12,13] plays an essential role in inflammatory responses. We previously established an LPS-responsive macrophage cell clone (RAW264.7/Luc-P1), in which NF-κB activity correlates with the luciferase gene expression [23]. The RAW 264.7/Luc-P1 cells allowed us to successfully identify NF-κB-suppressing compounds such as fisetin and methyl isornate [24,25]. Therefore, we applied this system to measure the effects of isolated compounds on NF-κB activity, and their inhibitory activities (with inhibitory percentages) are summarized in Table 2. 13,14-Didehydroxyisoxantho-chymol (**2**) and sampsonione B (**3**) show significant inhibition of LPS-stimulated NF-κB activity (Figure 8A,B). Moreover, 13,14-didehydroxyisoxanthochymol (**2**) and sampsonione B (**3**) did not induce cytotoxicity against RAW 264.7/Luc-P1 cells after 24 h treatment (Figure 8C,D).

LPS-mediated NF-κB activation results in upregulation of pro-inflammatory molecules, such as NO, in macrophages [12,26]. Thus, NO generation is a hallmark of inflammatory responses. Our study further evaluated the potential anti-inflammatory compounds, 13,14-didehydroxy- isoxanthochymol (**2**) and sampsonione B (**3**) on NO production. The result showed that 13,14-didehydroxyisoxanthochymol (**2**) did not obviously affect LPS-induced NO generation in RAW264.7 macrophages and did not display cytotoxicity against RAW 264.7 cells after 24 h treatment (Figure 9A,C). In contrast, sampsonione B (**3**) could suppress LPS-induced NO generation in a concentration-dependent manner (Figure 9B) without causing significant cytotoxicity (Figure 9D).

It is observed that the inhibition on NO production is in a close correlation with NF-κB activation (e.g. compound **3** in Figures 8B and 9B). Thus, compound **3** may be involved in NF-κB-dependent NO regulation.
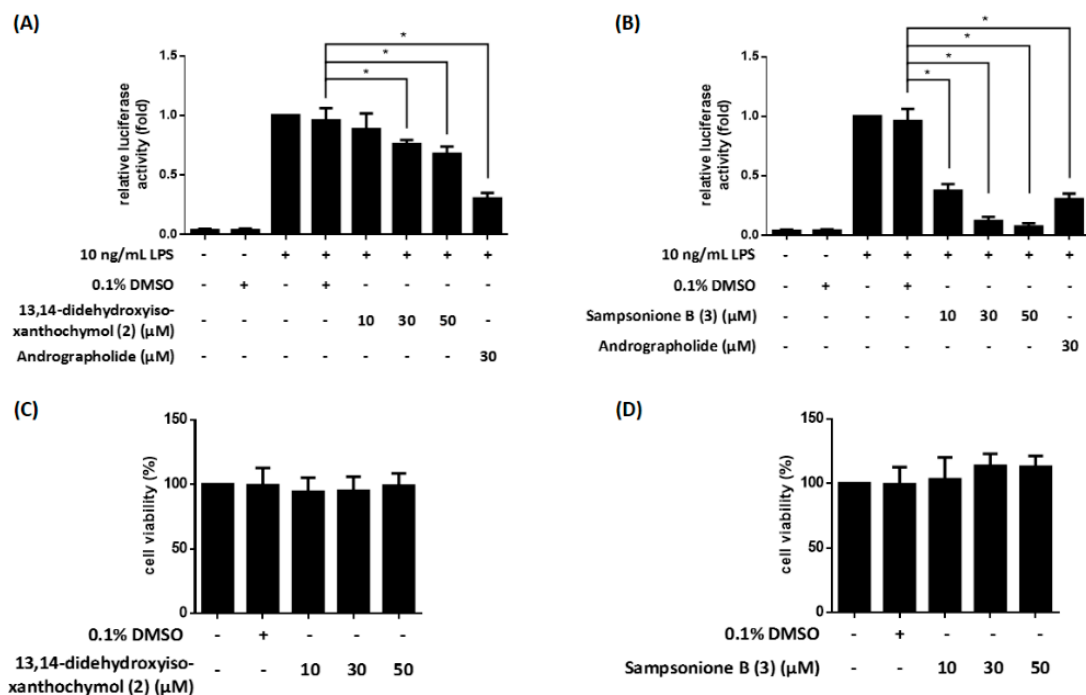
Figure 8. The compounds **2** and **3** inhibit NF-κB activation in lipopolysaccharide (LPS)-induced RAW 264.7/Luc-P1 cells. The luciferase activities of 13,14-didehydroxyisoxanthochymol (**2**) (**A**) and sampsonione B (**3**) (**B**) in LPS-stimulated RAW 264.7/Luc-P1 macrophages were observed. Andrographolide is the positive control. The cell viability of RAW 264.7/Luc-P1 cells incubated with 13,14-didehydroxyisoxanthochymol (**2**) (**C**) or sampsonione B (**3**) (**D**) for 24 h was measured using MTT assay. * indicates significant difference vs. LPS-treated vehicle control ($p < 0.05$).
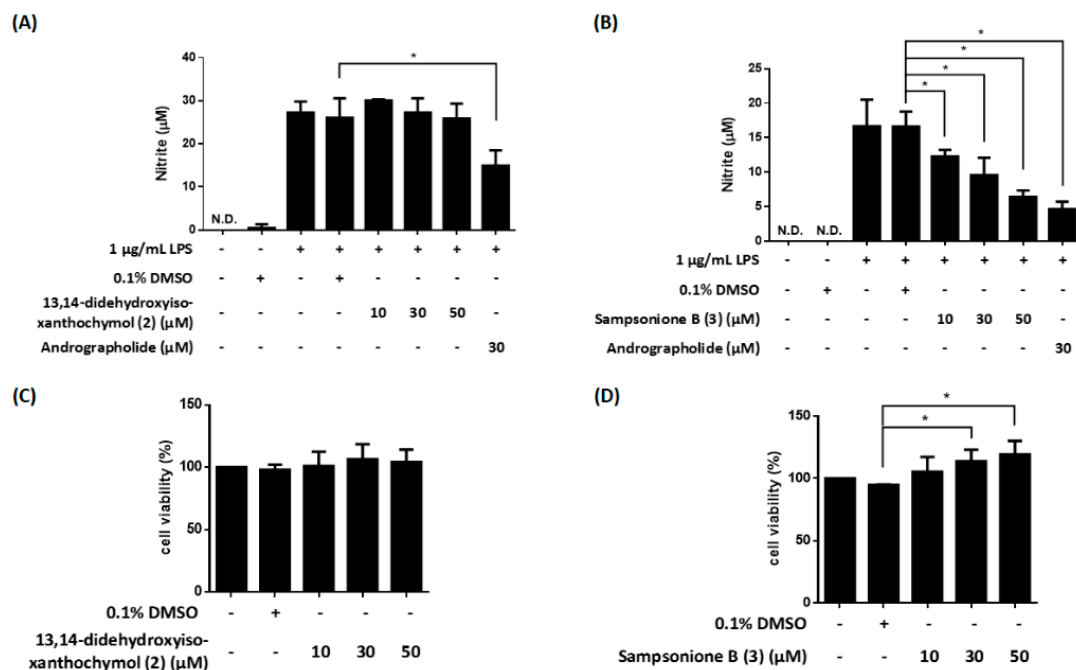

Figure 9. The effects of compounds **2** and **3** on nitric oxide (NO) production in LPS-induced RAW 264.7 macrophages. The effects of 13,14-didehydroxyisoxanthochymol (**2**) (**A**) and sampsonione B (**3**) (**B**) in LPS-treated RAW 264.7 macrophages were detected by Griess reagent. Andrographolide is the positive control. The cell viability of RAW 264.7 cells incubated with 13,14-didehydroxy- isoxanthochymol (**2**) (**C**) or sampsonione B (**3**) (**D**) for 24 h was measured using MTT assay. * indicates significant difference vs. LPS-treated vehicle control ($p < 0.05$).

Table 2. The effects of compounds **1**–**7** from the stems of *Garcinia multiflora* on NF-κB activation in RAW 264.7/Luc-P1 cells.

Compounds [a]	Relative Luciferase Activity	Inhibition (%) [e]
	Mean $\pm$ SD [d]	Mean $\pm$ SD [d]
13,14-Didehydroxygarcicowin C (**1**)	0.78 $\pm$ 0.11	21 $\pm$ 11
13,14-Didehydroxyisoxanthochymol (**2**)	0.75 $\pm$ 0.03 *	24 $\pm$ 4 *
Sampsonione B (**3**)	0.12 $\pm$ 0.03 *	88 $\pm$ 4 *
Garcinol (**4**)	1.23 $\pm$ 0.21	
3-Hydroxy-5-methoxybiphenyl (**5**)	0.85 $\pm$ 0.06	14 $\pm$ 3
1,24-Tetracosanediol diferulate (**6**)	0.96 $\pm$ 0.08	3 $\pm$ 10
Friedelan-3-one (**7**)	1.04 $\pm$ 0.20	
LPS-treated vehicle control [b]	0.94 $\pm$ 0.09	5 $\pm$ 9
Andrographolide [c]	0.31 $\pm$ 0.05 *	70 $\pm$ 5 *

[a] Compounds **1**–**7**: 30 μM. [b] Vehicle control: 0.1% DMSO. [c] Andrographolide (30 μM) is the positive control. [d] Data are displayed as the mean $\pm$ SD from three independent experiments. * indicates significant difference versus lipopolysaccharide (LPS) (1 μg/mL)-treated vehicle control ($p < 0.05$). [e] Inhibition (%) = [1 − luciferase activity (compounds)/luciferase activity (LPS-treated control)] $\times$ 100.

3. Experimental Section

3.1. General Procedures

Ultraviolet (UV) spectra were measured on a Jasco UV-240 spectrophotometer (Jasco Co., Hachioji, Japan). Optical rotations were measured using a Jasco DIP-370 polarimeter (Jasco Co., Hachioji, Japan) in MeOH. CD spectra were obtained on a Jasco J-815 spectropolarimeter (Jasco Co., Hachioji, Japan). Infrared (IR) spectra (neat or KBr) were determined on a Perkin Elmer 2000 FT-IR spectrometer (Perkin-Elmer Corp., Waltham, MA, USA). Nuclear magnetic resonance (NMR) spectra, including nuclear Overhauser effect spectrometry (NOESY), correlation spectroscopy (COSY), heteronuclear single-quantum coherence (HSQC), and heteronuclear multiple-bond correlation (HMBC) experiments, were measured on a Varian Inova 500 spectrometer (Varian, Palo Alto, CA, USA) operating at 125 MHz (^{13}C) and 500 MHz (^{1}H), respectively, with chemical shifts given in ppm (δ) using tetramethylsilane (TMS) as an internal standard. Electrospray ionization (ESI) and high-resolution electrospray ionization (HRESI)-mass spectra were determined on a Bruker APEX II mass spectrometer (Bruker, Billerica, MA, USA). Silica gel 60 F-254 (Merck, Darmstadt, Germany) was used for preparative thin-layer chromatography (PTLC) and thin-layer chromatography (TLC). Silica gel (70–230 and 230–400 mesh, Merck) was used for column chromatography (CC).

3.2. Plant Material

The stems of *G. multiflora* was collected from Mudan, Pingtung County, Taiwan, in December 2012 and identified by Dr. M. H. Yen (School of Pharmacy, College of Pharmacy, Kaohsiung Medical University, Taiwan). A voucher specimen (GM-201212) was deposited in the Faculty of Pharmacy, School of Pharmaceutical Sciences, National Yang-Ming University, Taipei, Taiwan.

3.3. Extraction and Isolation

The dried stems of *G. multiflora* (5.4 kg) were extracted three times with MeOH (10 L each) for 3 days. The MeOH extracts were concentrated under reduced pressure at 35 °C, and the residue (211 g) was partitioned between EtOAc and H$_2$O (1:1). The EtOAc layer was concentrated to give a residue (fraction A, 118 g). The water layer was further extracted with *n*-BuOH, and the water-soluble part (fraction C, 41 g) and the *n*-BuOH-soluble part (fraction B, 45 g) were separated. Fraction A (118 g) was separated on silica gel (70–230 mesh, 5.2 kg), eluting with CH$_2$Cl$_2$, gradually increasing the polarity with MeOH to give 13 fractions: A1 (2 L, CH$_2$Cl$_2$), A2 (2 L, CH$_2$Cl$_2$/MeOH, 90:1), A3 (2 L, CH$_2$Cl$_2$/MeOH, 80:1), A4 (1 L, CH$_2$Cl$_2$/MeOH, 50:1), A5 (1 L, CH$_2$Cl$_2$/MeOH, 40:1), A6 (2 L, CH$_2$Cl$_2$/MeOH, 30:1), A7 (2 L, CH$_2$Cl$_2$/MeOH, 20:1), A8 (5 L, CH$_2$Cl$_2$/MeOH, 10:1),

A9 (7 L, CH$_2$Cl$_2$/MeOH, 5:1), A10 (2 L, CH$_2$Cl$_2$/MeOH, 4:1), A11 (4 L, CH$_2$Cl$_2$/MeOH, 2:1), A12 (5 L, CH$_2$Cl$_2$/MeOH, 1:1), and A13 (5 L, MeOH).

Fraction A2 (5.6 g) was chromatographed further on silica gel (70–230 mesh, 250 g) eluting with *n*-hexane/acetone (20:1–0:1) to give 10 fractions (each 1.2 L, A2-1−A2-10). Compound **7** (7.2 mg) was yielded from fraction A2-1 (85 mg) by recrystallization with *n*-hexane/EtOAc. Compounds **8** and **9** (12.2 mg) were obtained from fraction A2-2 (358 mg) by recrystallization with *n*-hexane/EtOAc. Fraction A2-4 (126 mg) was purified further by preparative TLC (silica gel, CH$_2$Cl$_2$) to obtain **1** (5.2 mg) and **2** (2.3 mg). Part (168 mg) of fraction A2-5 was purified by preparative TLC (silica gel, *n*-hexane/EtOAc, 6:1) to obtain **3** (2.2 mg). Part (120 mg) of fraction A2-7 was purified by preparative TLC (silica gel, *n*-hexane/EtOAc, 3:1) to afford **5** (2.2 mg). Part (89 mg) of fraction A2-9 was purified by preparative TLC (silica gel, CHCl$_3$) to obtain **6** (2.5 mg). Fraction A3 (4.5 g) was chromatographed further on silica gel (230–400 mesh, 205 g) eluting with *n*-hexane/EtOAc (15:1–0:1) to give 7 fractions (each 1 L, A3-1–A3-7). Part (172 mg) of fraction A3-5 was purified by preparative TLC (silica gel, *n*-hexane/acetone, 2:1) to afford **4** (6.2 mg).

13,14-didehydroxygarcicowin C (**1**): amorphous powder; $[\alpha]_D^{25}$ = −68.6 (*c* 0.18, CHCl$_3$); CD (MeOH, $\Delta\varepsilon$): 311 (+2.1), 267 (−8.5), 223 (+5.2) nm; UV (MeOH): λ_{max} (log ε) = 250 (3.90), 273 (sh, 3.77) nm; IR (KBr): ν_{max} = 1729 (C=O), 1682 (C=O), 1645 (C=O) cm^{-1}; ESI-MS: *m/z* = 569 [M + H]$^+$; HR-ESI-MS: *m/z* = 569.36284 [M + H]$^+$ (calcd for C$_{38}$H$_{49}$O$_4$, 569.36254); ^{1}H and ^{13}C NMR data: see Table 1.

13,14-didehydroxyisoxanthochymol (**2**): amorphous powder; $[\alpha]_D^{25}$ = +205.7 (*c* 0.15, CHCl$_3$); CD (MeOH, $\Delta\varepsilon$): 270 (+13.6), 224 (−8.4) nm; UV (MeOH): λ_{max} (log ε) = 203 (4.16), 249 (3.96), 276 (sh, 4.02) nm; IR (KBr): ν_{max} = 1724 (C=O), 1675 (C=O), 1637 (C=O) cm^{-1}; ESI-MS: *m/z* = 571 [M + H]$^+$; HR-ESI-MS: *m/z* = 571.37822 [M + H]$^+$ (calcd for C$_{38}$H$_{51}$O$_4$, 571.37819); ^{1}H and ^{13}C NMR data: see Table 1.

3.4. Biological Assay

The effect of the isolates on LPS-induced NF-κB activation in RAW 264.7/Luc-P1 macrophage was assessed by determining the luminescence resulted from luciferase activity in a concentration- dependent manner. The purity of the tested compounds was >98% as identified by MS and NMR.

3.4.1. Cells and Culture Medium

The RAW 264.7/Luc-P1 cell is an LPS-responsive cell line with an integrated reporter gene (pELAM1-Luc) [23]. The murine RAW 264.7 macrophage and RAW 264.7/Luc-P1 cells were cultured and originated conditions as described previously [23,24].

3.4.2. Luciferase Reporter Assay

The RAW 264.7/Luc-P1 cells (1.5 × 10^5 cells in 24-well plates) were treated with pure compounds, the positive control (30 μM andrographolide) or vehicle (0.1% DMSO) for 1 h and then LPS (10 ng/mL) for 23 h. The treated cells were then collected and assessed using luciferase assays (Promega, Madison, WI, USA) as described previously [25].

3.4.3. 3-(4,5-Dimethylthiazol-2-yl)-2,5-diphenyltetrazolium Bromide (MTT) Assay

RAW 264.7/Luc-P1 cells or RAW 264.7 cells (10^4 cells in 96-well plates) were treated with 13,14-didehydroxyisoxanthochymol (**2**), sampsonione B (**3**) and 0.1% DMSO for 24 h. MTT assays were performed as described previously [25].

3.4.4. Nitric Oxide (NO) Production

The RAW 264.7 cells (4 × 10^4 cells in 96-well plates) were treated with 13,14-didehydroxy-isoxanthochymol (**2**), sampsonione B (**3**) and 0.1% DMSO for 1 h and then incubated with LPS (1μg/mL) for 23 h. The 100 μL of cell culture medium with an equal volume of Griess reagent (0.1% naphthylethylenediamine dihydrochloride and 1% sulfanilamide in 2.5% phosphoric acid) in a

96-well plate was incubated for 10 min. The absorbance at 550 nm was measured by using a Model 680 Microplate Reader (Bio-rad, Hercules, CA, USA). The level of NO production was calculated from sodium nitrite ($NaNO_2$) standard curve [27].

3.4.5. Statistical Analysis

The data are displayed as mean $\pm$ SD from three independent experiments. Statistical analysis was performed using Student's t test. Differences were considered as statistically significant when $p < 0.05$.

4. Conclusions

Our research on the phytochemical investigation of *G. multiflora* has led to the isolation of two new (**1**, **2**) and seven known (**3**–**9**) compounds. The structures of these isolates were established by spectroscopic data. Based on the results of our bioactivity assays, among the isolates, 13,14-didehydroxyisoxanthochymol (**2**) and sampsonione B (**3**) exhibited inhibition against lipopolysaccharide (LPS)-induced NF-κB activation in macrophages at 30 μM with relative luciferase activity values of 0.75 ± 0.03 and 0.12 ± 0.03, respectively. Furthermore, sampsonione B (**3**) showed LPS-induced NO generation in concentration dependent manner. Thus, our research suggests *G. multiflora* and its isolated compound (especially **3**) are worth further study and may be expectantly developed as the candidates for the prevention or treatment of diverse inflammatory diseases.

Supplementary Materials: Supplementary materials are available online, Figures S1–S8: MS, 1D, and 2D-NMR spectra for 13,14-didehydroxygarcicowin C (**1**), Figures S9–S16: MS, 1D, and 2D-NMR spectra for 13,14-didehydroxyisoxanthochymol (**2**).

Author Contributions: L.-Y.C. and J.-J.C. performed the isolation and structure elucidation of the constituents and manuscript writing. Y.-C.T., S.-L.F., M.-I.C., M.-J.C. and P.-J.S. conducted the bioassay and analyzed the data. J.-J.C. planned, designed, and organized all of the research of this study and the preparation of the manuscript. All authors read and approved the final version of the manuscript.

Conflicts of Interest: The authors declare no conflict of interest.

References

1. Robson, N.K.B. *'Guttiferae' in 'Flora of Taiwan'*, 2nd ed.; Editorial Committee of the Flora of Taiwan: Taipei, Taiwan, 1996; Volume 2, pp. 694–714.
2. Mohamed, G.A.; Ibrahim, S.R.M.; Shaaban, M.I.A.; Ross, S.A. Mangostanaxanthones I and II, new xanthones from the pericarp of *Garcinia mangostana*. *Fitoterapia* **2014**, *98*, 215–221. [CrossRef] [PubMed]
3. Sukandar, E.R.; Ersam, T.; Fatmawati, S.; Siripong, P.; Aree, T.; Tip-pyang, S. Cylindroxanthones A–C, three xanthones and their cytotoxicity from the stem bark of *Garcinia cylindrocarpa*. *Fitoterapia* **2016**, *108*, 62–65. [CrossRef] [PubMed]
4. Sukandar, E.R.; Siripong, P.; Khumkratok, S.; Tip-pyang, S. New depsidones and xanthone from the roots of *Garcinia schomburgkiana*. *Fitoterapia* **2016**, *111*, 73–77. [CrossRef] [PubMed]
5. Tang, Z.Y.; Xia, Z.X.; Qiao, S.P.; Jiang, C.; Shen, G.R.; Cai, M.X.; Tang, X.Y. Four new cytotoxic xanthones from *Garcinia nujiangensis*. *Fitoterapia* **2015**, *102*, 109–114. [CrossRef] [PubMed]
6. Chen, J.J.; Ting, C.W.; Hwang, T.L.; Chen, I.S. Benzophenone derivatives from the fruits of *Garcinia multiflora* and their anti-inflammatory activity. *J. Nat. Prod.* **2009**, *72*, 253–258. [CrossRef] [PubMed]
7. Weng, J.R.; Tsao, L.T.; Wang, J.P.; Wu, R.R.; Lin, C.N. Anti-inflammatory phloroglucinols and terpenoids from *Garcinia subelliptica*. *J. Nat. Prod.* **2014**, *67*, 1796–1799. [CrossRef] [PubMed]
8. Weng, J.R.; Lin, C.N.; Tsao, L.T.; Wang, J.P. Novel and anti-inflammatory constituents of *Garcinia subelliptica*. *Chem. Eur. J.* **2003**, *9*, 1958–1963. [CrossRef] [PubMed]

9.　Wu, C.C.; Lu, Y.H.; Wei, B.L.; Yang, S.C.; Won, S.J.; Lin, C.N. Phloroglucinols with prooxidant activity from *Garcinia subelliptica*. *J. Nat. Prod.* **2008**, *71*, 246–250. [CrossRef] [PubMed]

10.　Tan, W.N.; Khairuddean, M.; Wong, K.C.; Khaw, K.Y.; Vikneswaran, M. New cholinesterase inhibitors from *Garcinia atroviridis*. *Fitoterapia* **2014**, *97*, 261–267. [CrossRef] [PubMed]

11.　Killeen, M.J.; Linder, M.; Pontoniere, P.; Crea, R. NF-κB signaling and chronic inflammatory diseases: Exploring the potential of natural products to drive new therapeutic opportunities. *Drug Discov. Today* **2014**, *19*, 373–378. [CrossRef] [PubMed]

12.　Karin, M.; Clevers, H. Reparative inflammation takes charge of tissue regeneration. *Nature* **2016**, *529*, 307–315. [CrossRef] [PubMed]

13.　Riedel, C.U.; Foata, F.; Philippe, D.; Adolfsson, O.; Eikmanns, B.J.; Blum, S. Anti-inflammatory effects of bifidobacteria by inhibition of LPS-induced NF-κB activation. *World J. Gastroenterol.* **2006**, *12*, 3729–3735. [CrossRef] [PubMed]

14.　Xu, G.; Kan, W.L.T.; Zhou, Y.; Song, J.Z.; Han, Q.B.; Qiao, C.F.; Cho, C.H.; Rudd, J.A.; Lin, G.; Xu, H.X. Cytotoxic acylphloroglucinol derivatives from the twig of *Garcinia cowa*. *J. Nat. Prod.* **2010**, *73*, 104–108. [CrossRef] [PubMed]

15.　Stark, T.D.; Lösch, S.; Wakamatsu, J.; Balemba, O.B.; Frank, O.; Hofmann, T. UPLC-ESI-TOF MS-based metabolite profiling of the antioxidative food supplement *Garcinia buchananii*. *J. Agric. Food Chem.* **2015**, *63*, 7169–7179. [CrossRef] [PubMed]

16.　Socolsky, C.; Plietker, B. Total synthesis and absolute configuration assignment of MRSA active garcinol and isogarcinol. *Chem. Eur. J.* **2015**, *21*, 3053–3061. [CrossRef] [PubMed]

17.　Hu, L.H.; Sim, K.Y. Complex caged polyisoprenylated benzophenone derivatives, sampsonione A and B, from *Hypericum sampsonii*. *Tetrahedron Lett.* **1998**, *39*, 7999–8002. [CrossRef]

18.　Song, M.C.; Nigussie, F.; Jeong, T.S.; Lee, C.Y.; Regassa, F.; Markos, T.; Baek, N.I. Phenolic compounds from the roots of *Lindera fruticosa*. *J. Nat. Prod.* **2006**, *69*, 853–855. [CrossRef] [PubMed]

19.　Ma, C.Y.; Liu, W.K.; Che, C.T. Lignanamides and nonalkaloidal components of *Hyoscyamus niger* seeds. *J. Nat. Prod.* **2002**, *65*, 206–209. [CrossRef] [PubMed]

20.　Hisham, A.; Jaya Kumar, G.; Fujimoto, Y.; Hara, N. Salacianone and salacianol, two triterpenes from *Salacia beddomei*. *Phytochemistry* **1995**, *40*, 1227–1231. [CrossRef]

21.　Ibrahimm, S.R.M.; Elkhayat, E.S.; Mohamed, G.A.; Khedr, A.I.M.; Fouad, M.A.; Kotb, M.H.R.; Ross, S.A. Aspernolides F and G, new butyrolatones from the endophytic fungus *Aspergillus terreus*. *Phytochemistry Lett.* **2015**, *14*, 84–90. [CrossRef]

22.　Monção, N.B.N.; Araújo, B.Q.; do Nascimento Silva, J.; Lima, D.J.B.; Ferreira, P.M.P.; da Silva Airoldi, F.P.; Pessoa, C.; das, G.L.; Citó, A.M. Assessing chemical constituents of *Mimosa caesalpiniifolia* stem bark: Possible bioactive components accountable for the cytotoxic effect of *M. caesalpiniifolia* on human tumour cell lines. *Molecules* **2015**, *20*, 4204–4224. [CrossRef] [PubMed]

23.　Fu, S.L.; Hsu, H.Y.; Lee, P.Y.; Hou, W.C.; Hung, C.L.; Lin, C.H.; Chen, C.M.; Huang, Y.J. Dioscorin isolated from *Dioscorea alata* activates TLR4-signaling pathways and induces cytokine expression in macrophages. *Biochem. Biophys. Res. Commun.* **2006**, *339*, 137–144. [CrossRef] [PubMed]

24.　Liu, S.H.; Lin, C.H.; Hung, S.K.; Chou, J.H.; Chi, C.W.; Fu, S.L. Fisetin inhibits liopolysaccharide-induced macrophage activation and dendritic cell maturation. *J. Agric. Food Chem.* **2010**, *58*, 10831–10839. [CrossRef] [PubMed]

25.　Tsai, Y.C.; Chen, S.H.; Lin, L.C.; Fu, S.L. Anti-inflammatory principles from *Sarcandra glabra*. *J. Agric. Food Chem.* **2017**, *65*, 6497–6505. [CrossRef] [PubMed]

26.　MacMicking, J.; Xie, Q.W.; Nathan, C. Nitric oxide and macrophage function. *Ann. Rev. Immunol.* **1997**, *15*, 323–350. [CrossRef] [PubMed]

27.　Wang, S.L.; Tsai, Y.C.; Fu, S.L.; Cheng, M.J.; Chung, M.I.; Chen, J.J. 2-(2-Phenylethyl)-4*H*-chromen-4-one derivatives from the resinous wood of *Aquilaria sinensis* with anti-inflammatory effect in LPS-induced macrophages. *Molecules* **2018**, *23*, 289. [CrossRef] [PubMed]

Sample Availability: Samples of the compounds are available from the authors.